Hindawi
Mathematical Problems in Engineering
Volume 2018, Article ID 4371585, 12 pages
https://doi.org/10.1155/2018/4371585

Research Article

Rocking Response Analysis of Self-Centering Walls under Ground Excitations

Xiaobin Hu, Qinwang Lu, and Yang Yang

School of Civil Engineering, Wuhan University, Wuhan 430072, China

Correspondence should be addressed to Xiaobin Hu; newhxb@126.com

Received 17 November 2017; Revised 30 January 2018; Accepted 18 February 2018; Published 20 March 2018

Academic Editor: Angelo Di Egidio

This paper presents a numerical procedure to simulate the rocking response of self-centering walls under ground excitations. To this aim, the equations of motion that govern the dynamic response of self-centering walls are first formulated and then solved numerically, in which three different self-centering wall structural systems are considered, that is, (i) including the self-weight of the wall only, (ii) including posttensioned tendon, and (iii) including both posttensioned tendon and dampers. Following the development of the numerical procedure, parametric studies are then carried out to investigate the influence of a variety of factors on the dynamic response of the self-centering wall under seismic excitations. The investigation results show that within the cases studied in this paper the installation of posttensioned tendon is capable of significantly enhancing the self-centering ability of the self-centering wall. In addition, increasing either the initial force or the elastic stiffness of the posttensioned tendon can reduce the dynamic response of the self-centering wall in terms of the rotation angle and angular velocity, whereas the former approach is found to be more effective than the latter one. It is also revealed that the addition of the dampers is able to improve the energy dissipation capacity of the self-centering wall. Furthermore, for the cases studied in this paper the yield strength of the dampers appears to have a more significant effect on the dynamic response of the self-centering wall than the elastic stiffness of the dampers.

1. Introduction

In performance-based earthquake engineering, the residual deformation of structures has been recognized as a complementary parameter in the evaluation of structural (and nonstructural) damage [1, 2]. As such, self-centering (SC) seismic resisting systems have attracted considerable research interests within the earthquake engineering community [3–9]. As a typical SC structure, the SC wall is mainly composed of three components: the wall, the posttensioned (PT) tendon, and the dampers. In contrast to conventional shear wall structures, the SC wall is anticipated to rock about the foundation by taking advantage of the gap-opening behavior of horizontal connections at the base or along the height of the wall.

In view of the significance of SC walls, a number of studies on the static and dynamic performance of SC walls have been carried out mainly through numerical and experimental methodologies. For instance, Kurama et al. [10–12] put forward a seismic design approach for SC precast concrete walls and established an analytical model using fiber beam-column elements in DRAIN-2DX to investigate its seismic performance. Subsequently, Perez [13] developed a trilinear idealized base shear-lateral drift response curve for SC precast concrete walls under monotonic lateral loading and conducted experiments consisting of five SC precast concrete walls under combined gravity and lateral loads. Furthermore, Toranzo et al. [14, 15] proposed a SC confined masonry wall and conducted shake-table experimental tests. The author also constructed a numerical model for the SC confined masonry wall, in which the wall is modeled by diagonal struts and the rocking behavior at the base is simulated by a group of contact springs. In a different way, Belleri et al. [16] performed finite element modeling of rocking walls in order to highlight the differences between different modeling techniques comprising 3D, 2D, and 1D elements using nonlinear static and dynamic analysis approaches. The finite element models considered in their study adopt nonlinear brick and plane-stress plate elements, fiber beam elements, compression only springs, and concentrated rotational springs. In addition to

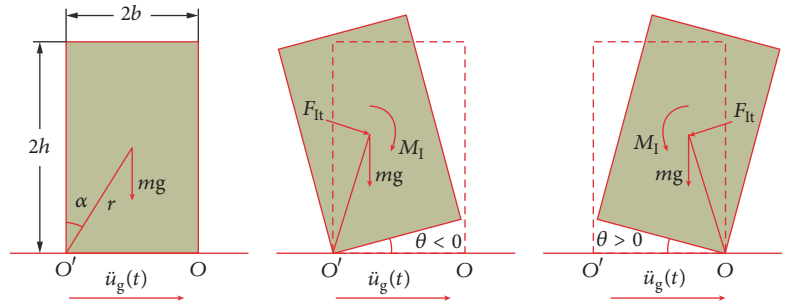

(a) Original position (b) Rotating about O' (c) Rotating about O

FIGURE 1: Mechanical analysis of the SC wall considering only its self-weight.

the above-mentioned studies, a number of research works have also been reported in [17–25], concerning a variety of the experimental, numerical, or analytical investigations on the mechanical or seismic performance of SC walls.

In general, the analytical and numerical models of SC walls in the above-mentioned studies can be classified into two categories. One category involves using structural elements such as beam, truss, and spring elements, which is normally exploited in research-based structural analysis programs such as DRAIN-2DX and OpenSees. The other category, which is commonly adopted in general-purpose finite element software packages such as ANSYS and ABAQUS, utilizes 2D or 3D elements to model the wall and contact elements to simulate the interaction between the wall and the foundation. It is however noted that although these two types of numerical models are able to realistically simulate the structural behavior of SC walls, it is difficult to determine the parameters related to the springs or the contact elements.

Similar to SC walls, rigid structures such as electrical equipment might also enter into rocking motion under strong ground shaking that occasionally results in overturning. Considerable studies pertaining to the rocking response of the rigid blocks can be found in the literatures (e.g., among others, [26–35]). In these studies, the rocking responses of rigid blocks are investigated both theoretically and numerically considering different ground excitations. Motivated by these works, this paper presents a numerical analysis approach to investigate the dynamic behavior of SC walls subjected to ground excitations. To address the issue, the equations of motion that govern the rocking response of three different SC wall structural systems are first formulated and then solved numerically, which include (i) considering the self-weight of the wall only, (ii) considering PT tendon, and (iii) considering both PT tendon and dampers. After that, parametric studies are then conducted to examine the influences of a variety of factors on the dynamic behavior of the SC wall under seismic excitations.

2. Rocking Response of the SC Wall under Self-Weight Only

2.1. General Description of the Problem. For the convenience of theoretical derivation, the wall is treated as a rigid body since this assumption was widely adopted in the aforementioned literatures [10, 13, 15]. In addition, the slab carried by the wall is ignored although its mass can be lumped to the SC wall in order to consider its inertia effect. The configuration of the wall at the initial position is shown in Figure 1(a), where $2h$, $2b$, and r represent the height, the width, and half the length of the diagonal, respectively, and α is the angle between the height of the wall and the diagonal of the wall. In the meantime, mg indicates the self-weight of the wall, while $\ddot{u}_g$ denotes the acceleration of the ground motion, which has the positive direction shown in Figure 1(a). It is assumed that when subjected to ground excitations, the SC wall only rocks without sliding, as seen in Figures 1(b) and 1(c), where θ is the rotation angle of the SC wall, which is supposed to be positive for the wall rotating about point O and negative in case of rotating about O'.

2.2. Equation of Motion

2.2.1. Rotating about O'. When the wall rotates about O', as seen in Figure 1(b), the tangential inertial force F_{It} and the inertial moment M_I are

$$\begin{aligned} F_{It} &= m\left\{-\ddot{\theta}(t)\, r - \ddot{u}_g(t)\cos\left[\alpha+\theta(t)\right]\right\} \\ M_I &= -I_{cg}\ddot{\theta}(t), \end{aligned} \tag{1}$$

where $I_{cg} = mr^2/3$ is the moment of inertia of the wall about its centroid. According to the D'Alembert principle, the following moment equilibrium equation can be established

$$\begin{aligned} &I_0\ddot{\theta}(t) + mgr\sin\left[-\alpha-\theta(t)\right] \\ &\quad = -m\ddot{u}_g(t)\, r\cos\left[-\alpha-\theta(t)\right], \end{aligned} \tag{2}$$

where $I_0 = I_{cg}+mr^2$ is the moment of inertia of the wall about point O'.

2.2.2. Rotating about O. When the wall rotates about O, as shown in Figure 1(c), F_{It} and M_I become

$$\begin{aligned} F_{It} &= m\left\{\ddot{\theta}(t)\, r + \ddot{u}_g(t)\cos\left[\alpha-\theta(t)\right]\right\} \\ M_I &= I_{cg}\ddot{\theta}(t). \end{aligned} \tag{3}$$

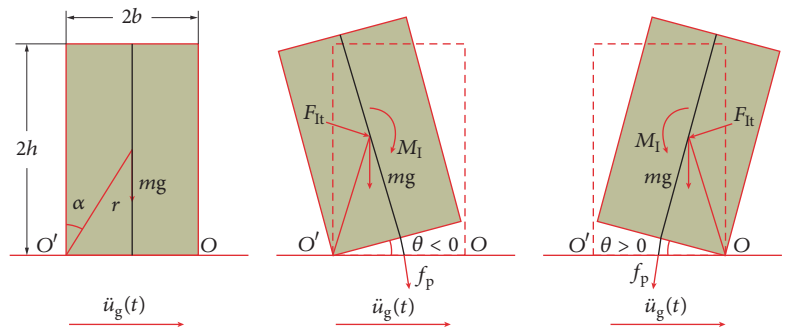

(a) Original position (b) Rotating about O' (c) Rotating about O

FIGURE 2: Mechanical analysis of the SC wall including the PT tendon.

Similarly, the following moment equilibrium equation can be achieved

$$I_0\ddot{\theta}(t) + mgr\sin[\alpha - \theta(t)] = -m\ddot{u}_g(t)\, r\cos[\alpha - \theta(t)]. \tag{4}$$

2.3. Linearization of the Equation of Motion. Eqs. (2) and (4) form the governing equations of motion of the SC wall under seismic excitations. To derive the analytical solutions, the equations need to be further linearized. Assuming that the rotation of the wall is sufficiently small leads to the following approximation

$$-\alpha - \theta(t) \approx -\alpha, \quad \alpha - \theta(t) \approx \alpha \tag{5a}$$

$$\cos\frac{\theta(t)}{2} \approx 1, \quad \sin\theta(t) \approx \theta(t). \tag{5b}$$

Furthermore, sine excitation is adopted in the present study, that is,

$$\ddot{u}_g(t) = a_g \sin w_g t, \tag{6}$$

where a_g and w_g are the amplitude and exciting frequency of the excitation, respectively.

Substituting (5a), (5b), and (6) into (2) and (4) yields

$$\ddot{\theta}(t) = -\frac{a_g}{g}p^2\cos\alpha\sin w_g t + p^2\sin\alpha, \quad \theta < 0 \tag{7a}$$

$$\ddot{\theta}(t) = -\frac{a_g}{g}p^2\cos\alpha\sin w_g t - p^2\sin\alpha, \quad \theta > 0, \tag{7b}$$

where $p = \sqrt{3g/(4r)}$.

The following initial condition is assumed

$$\theta(0) = \theta_0, \quad \dot{\theta}(0) = \dot{\theta}_0, \tag{8}$$

where θ_0 and $\dot{\theta}_0$ are the initial rotation angle and angular velocity of the SC wall. Combining (7a), (7b), and (8) yields

$$\theta(t) = \frac{1}{2}\sin\alpha\,(pt)^2 + \frac{a_g}{g}\left(\frac{p}{w_g}\right)^2\cos\alpha\sin w_g t + C_1 t + C_2, \quad \theta < 0 \tag{9a}$$

$$\theta(t) = -\frac{1}{2}\sin\alpha\,(pt)^2 + \frac{a_g}{g}\left(\frac{p}{w_g}\right)^2\cos\alpha\sin w_g t + C_3 t + C_4, \quad \theta > 0, \tag{9b}$$

where

$$C_1 = C_3 = \dot{\theta}_0 - \frac{a_g}{g}\frac{p^2}{w_g}\cos\alpha \tag{10a}$$

$$C_2 = C_4 = \theta_0. \tag{10b}$$

3. Rocking Response of the SC Wall with PT Tendon

In order to study the influence of the PT tendon on the dynamic response of the SC wall under earthquake excitations, a PT tendon is incorporated into the SC wall system and placed along the vertical center line of the SC wall, as shown in Figure 2(a). It is also assumed that the PT tendon behaves in a linear elastic manner during the entire loading process which has been verified by a number of experimental studies concerning SC walls [20, 23, 24]. For convenience, the wall is still assumed to be a rigid body neglecting the deformation concentrating on the contact region between the wall and the PT tendon [21].

3.1. Equation of Motion

3.1.1. Rotating about Point O'. When the wall rotates about point O', as shown in Figure 2(b), the force f_p in the PT tendon is

$$f_p = f_{p0} - 2k_p b\sin\frac{\theta(t)}{2}, \tag{11}$$

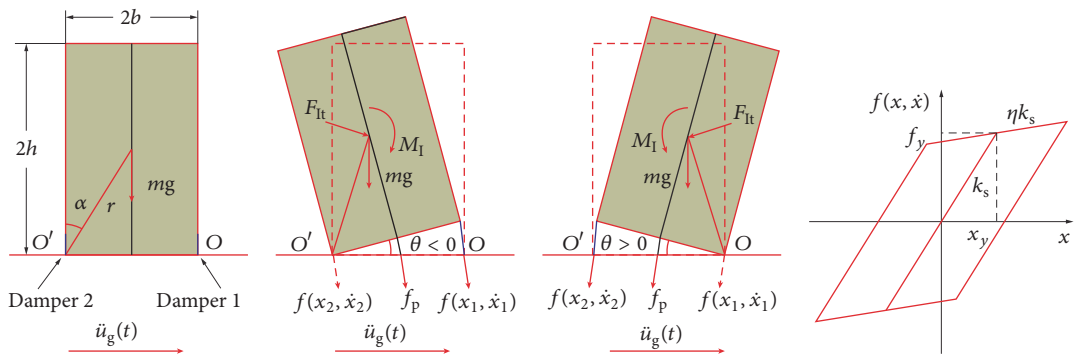

(a) Original position (b) Rotating about O' (c) Rotating about O (d) Hysteresis model of the damper

FIGURE 3: Mechanical analysis of the SC wall including both the PT tendon and dampers.

where f_{p0} and k_p are the initial force and the elastic stiffness of the tendon, respectively.

According to the D'Alembert principle, the following moment equilibrium equation can be obtained

$$I_0\ddot{\theta}(t) + mgr\sin[-\alpha - \theta(t)] - f_{p0}b\cos\frac{\theta(t)}{2} + k_p b^2 \sin\theta(t) = -m\ddot{u}_g(t)\, r\cos[-\alpha - \theta(t)]. \tag{12}$$

3.1.2. Rotating about Point O. When the wall rotates about point O, as shown in Figure 2(c), the force in the PT tendon is

$$f_p = f_{p0} + 2k_p b\sin\frac{\theta(t)}{2}. \tag{13}$$

Accordingly, the moment equilibrium equation becomes

$$I_0\ddot{\theta}(t) + mgr\sin[\alpha - \theta(t)] + f_{p0}b\cos\frac{\theta(t)}{2} + k_p b^2 \sin\theta(t) = -m\ddot{u}_g(t)\, r\cos[\alpha - \theta(t)]. \tag{14}$$

3.2. Linearization of the Equation of Motion. Eqs. (12) and (14) constitute the governing equations of motion of the SC wall considering the PT tendon under ground excitations. For comparison purposes, the same sine excitation as in (6) and the small rotation assumption are still applied here. As a result, (12) and (14) can be recast as

$$\ddot{\theta}(t) + p^2\beta\theta(t) = -\frac{a_g}{g}p^2\cos\alpha\sin w_g t + p^2\gamma, \quad \theta < 0 \tag{15a}$$

$$\ddot{\theta}(t) + p^2\beta\theta(t) = -\frac{a_g}{g}p^2\cos\alpha\sin w_g t - p^2\gamma, \quad \theta > 0, \tag{15b}$$

where $\beta = k_p b^2/mgr$ and $\gamma = \sin\alpha + f_{p0}b/mgr$.

Considering the initial condition as in (8), the solution to (15a) and (15b) can be derived as

$$\theta(t) = C_1\cos\left(p\sqrt{\beta}t\right) + C_2\sin\left(p\sqrt{\beta}t\right) + \frac{\gamma}{\beta} - \frac{\cos\alpha}{\beta - w_g^2/p^2}\frac{a_g}{g}\sin w_g t, \quad \theta < 0 \tag{16a}$$

$$\theta(t) = C_3\cos\left(p\sqrt{\beta}t\right) + C_4\sin\left(p\sqrt{\beta}t\right) - \frac{\gamma}{\beta} - \frac{\cos\alpha}{\beta - w_g^2/p^2}\frac{a_g}{g}\sin w_g t, \quad \theta > 0, \tag{16b}$$

where

$$C_1 = \theta_0 - \frac{\gamma}{\beta} \tag{17a}$$

$$C_3 = \theta_0 + \frac{\gamma}{\beta} \tag{17b}$$

$$C_2 = C_4 = \frac{\dot{\theta}_0}{p\sqrt{\beta}} + \frac{\cos\alpha}{\sqrt{\beta}}\frac{(w_g/p)}{\beta - w_g^2/p^2}\frac{a_g}{g}. \tag{17c}$$

4. Rocking Response of the SC Wall considering Both the PT Tendon and Dampers

In this section, both the PT tendon and dampers are added to the SC wall, the objective of which is to study the influence of the dampers on the dynamic response of the SC wall under ground excitations. It is supposed that dampers are installed near the two ends of the wall bottom, as shown in Figure 3(a). The restoring forces of the two dampers are $f_1(x_1, \dot{x}_1)$ and $f_2(x_2, \dot{x}_2)$, respectively, as seen in Figure 3(b), where x_1 and x_2 represent the displacements of the two dampers and $\dot{x}_1$ and $\dot{x}_2$ represent the velocities of the dampers. The bilinear elastoplastic model is adopted to describe the hysteresis behavior of the dampers, as seen in Figure 3(d), where f_y, x_y, k_s, and η represent the yield force, the yield displacement,

the elastic stiffness, and the postyield stiffness coefficient, respectively.

4.1. Mathematic Description of the Hysteresis of the Damper. For the damper with bilinear hysteresis, the restoring force can be written as follows [36]

$$f(x,\dot{x}) = \eta k_s x + (1-\eta) k_s z \tag{18a}$$

$$\dot{z} = \dot{x}\left[1 - \varepsilon(\dot{x})\,\varepsilon\left(z - x_y\right) - \varepsilon(-\dot{x})\,\varepsilon\left(-z - x_y\right)\right], \tag{18b}$$

where z is the hysteresis displacement and $\varepsilon(\cdot)$ is the unit step function defined as follows

$$\varepsilon(x) = \begin{cases} 0, & x < 0 \\ 1, & x \geq 0. \end{cases} \tag{19}$$

It is noted that the above equations are applicable for the two dampers. When the wall rotates about point O', the displacements of the two dampers are

$$x_1 = -4b \sin\frac{\theta(t)}{2}. \tag{20a}$$

$$x_2 = 0 \tag{20b}$$

When the wall rotates about point O, the displacements are then changed to

$$x_1 = 0 \tag{21a}$$

$$x_2 = 4b \sin\frac{\theta(t)}{2}. \tag{21b}$$

4.2. Equation of Motion. When the wall rotates about point O', as shown in Figure 3(b), utilizing the D'Alembert principle, the following moment equilibrium equation can be obtained

$$\begin{aligned} &I_0\ddot{\theta}(t) + mgr\sin[-\alpha - \theta(t)] - f_{p0} b\cos\frac{\theta(t)}{2} \\ &\quad + k_p b^2 \sin\theta(t) - 2f_1(x,\dot{x})\, b\cos\frac{\theta(t)}{2} \\ &\quad = -m\ddot{u}_g(t)\, r\cos[-\alpha - \theta(t)]. \end{aligned} \tag{22}$$

On the other hand, in case of rotating about point O, as shown in Figure 3(c), the corresponding moment equilibrium equation is then expressed as

$$\begin{aligned} &I_0\ddot{\theta}(t) + mgr\sin[\alpha - \theta(t)] + f_{p0} b\cos\frac{\theta(t)}{2} \\ &\quad + k_p b^2 \sin\theta(t) + 2f_2(x,\dot{x})\, b\cos\frac{\theta(t)}{2} \\ &\quad = -m\ddot{u}_g(t)\, r\cos[\alpha - \theta(t)]. \end{aligned} \tag{23}$$

Eqs. (22) and (23) can be combined into the following compact form

$$\begin{aligned} \ddot{\theta}(t) = -p^2 \Bigg\{ &\sin[\alpha\ \ \mathrm{sgn}[\theta(t)] - \theta(t)] + \mathrm{sgn}[\theta(t)] \\ &\cdot \frac{f_{p0} b}{mgr}\cos\frac{\theta(t)}{2} + \frac{k_p b^2}{mgr}\sin\theta(t) \\ &+ \{\varepsilon[-\theta(t)]\, f_1(x,\dot{x}) + \varepsilon[\theta(t)]\, f_2(x,\dot{x})\} \\ &\cdot \mathrm{sgn}[\theta(t)]\,\frac{2b}{mgr}\cos\frac{\theta(t)}{2} + \frac{\ddot{u}_g}{g} \\ &\cdot \cos[\alpha\ \ \mathrm{sgn}[\theta(t)] - \theta(t)] \Bigg\}, \end{aligned} \tag{24}$$

where $\mathrm{sgn}(\cdot)$ is the sign function.

When the rotation angle of the SC wall reverses ($\theta = 0$), an impact between the wall and the foundation will take place. Supposing that the rotation varies smoothly during impact, the relationship between the angular velocity of the SC wall before impact and that after impact can be determined approximately through the conservation of momentum as follows [30]

$$I_0\dot{\theta}_1 - m\dot{\theta}_1 2br\sin\alpha = I_0\dot{\theta}_2, \tag{25}$$

where $\dot{\theta}_1$ and $\dot{\theta}_2$ are the angular velocity before and after impact. Manipulating (25) then gives

$$k = \frac{\dot{\theta}_2}{\dot{\theta}_1} = 1 - \frac{3}{2}\sin^2\alpha, \tag{26}$$

where k is the ratio of the angular velocity of the SC wall after impact to that before impact. It is noted that the value of k is generally smaller than 1.0, indicating the energy dissipation due to impact.

4.3. Numerical Simulation. Due to the highly nonlinear nature inherent in the aforementioned differential equations, the MATLAB/Simulink software [37] is employed to obtain the numerical solutions to the differential equations. The Simulink model is schematically shown in Figure 4, which is mainly composed of seven modules or subsystems in total, that is, the ground excitation module, the wall subsystem, the PT tendon subsystem, the damper subsystem, two integration modules, and the output module. The ground excitation module can be used to input various types of excitations such as harmonic excitation, pulse excitation, and seismic excitation. The parameters associated with the subsystems include (i) $2b$, $2h$, and m (the wall subsystem), (ii) f_{p0} and k_p (the PT tendon subsystem), and (iii) f_y and k_s, and η (the damper subsystem). The Integration 1 module is intended for simulating the impact between the SC wall and the foundation by modifying the angular velocity after impact through the Gain module. It is worth noting that the Simulink model can also be used to reproduce the dynamic responses of the SC wall under various circumstances provided that the

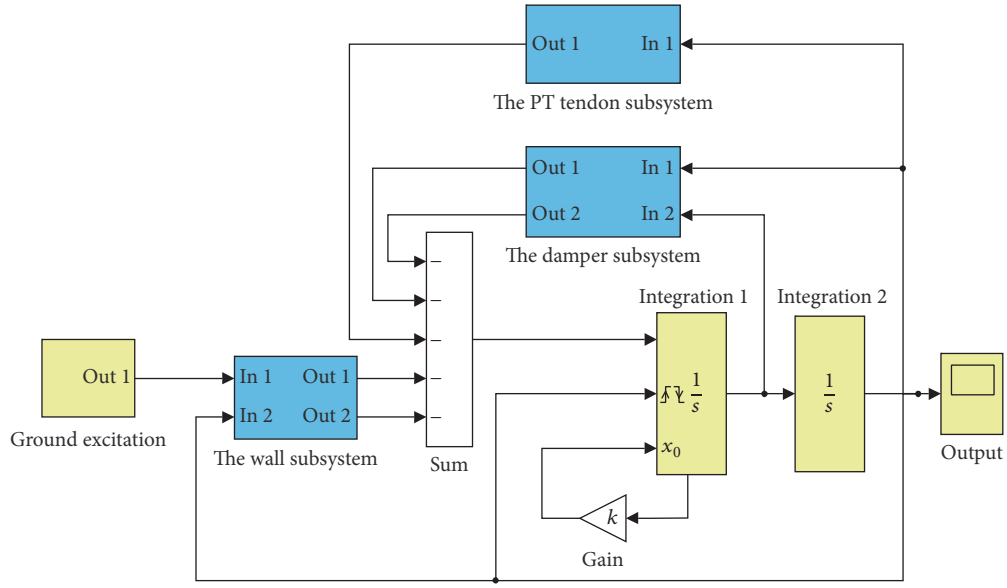

Figure 4: Simulink model of the SC wall under the ground excitation.

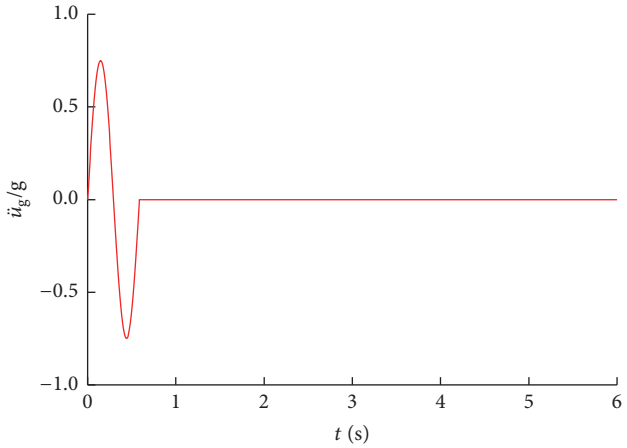

Figure 5: The sine pulse ground excitation.

corresponding subsystems are added or discarded. For example, if the PT tendon and damper subsystems are both deleted, the model can thus be applied to simulate the dynamic response of the SC wall considering only its self-weight.

To verify the validity and accuracy of the above model, the dynamic responses of the free-standing block under sine pulse excitation displayed in Figure 5 are computed and compared to those reported by Zhang and Makris [30]. In the verification, $\alpha = 0.25$ and $p = 2.14$ rad/s as well as other parameters are taken from their study. Figure 6 shows the computed time histories of rotation angle and angular velocity for the block. It can be seen that the simulated results agree well with those by Zhang and Makris, indicating that the Simulink model developed in this paper does a pretty good job in reproducing the response behavior of the standing block under ground excitations.

Table 1: Summary of parameters utilized in the numerical example.

	Parameters	Value
Wall panel	h (m)	1.5
	b (m)	0.5
	m (kg)	1176
PT tendon	f_{p0} (kN)	3.11
	k_p (kN/mm)	2.43
Sine excitation	a_g (g)	1.0
	w_g (rad/s)	4.8

5. Effect of the PT Tendon and Dampers on the Rocking Response of the SC Wall

The above sections give the equations governing the rocking responses of SC walls and the corresponding analytical and numerical solutions under three different cases. In this section, two examples are designed to investigate the influence of the PT tendon and dampers on the rocking responses of the SC wall, respectively.

5.1. Influence of the PT Tendon. To illustrate the influence of the PT tendon on the dynamic response of the SC wall, a numerical example is developed here, in which a sine excitation as defined in (6) is used. The amplitude of sine excitation a_g is intentionally set to 1.0g, which is large enough to topple the SC wall solely considering its self-weight according to the results given by Zhang and Makris [30]. It is assumed that the SC wall rotates about O' and has zero initial conditions, that is, $\theta_0 = \dot{\theta}_0 = 0$. Other relevant parameters considered in the example are given in Table 1.

Figure 7 displays time history curves of the rotation angle of the SC wall under the sine excitation before and

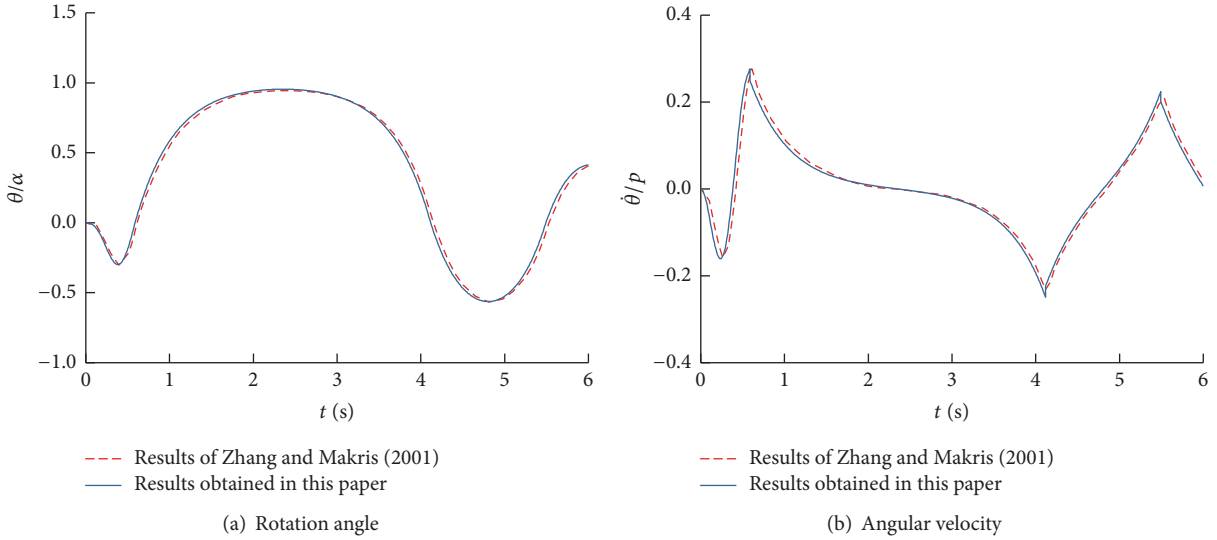

(a) Rotation angle (b) Angular velocity

Figure 6: Comparison of dynamic responses.

after adding the PT tendon obtained by (9a) and (16a) and Simulink simulation, respectively. It can be seen that the Simulink simulation results approach well with those from the theoretical linearization solutions especially under small rotation angle, verifying again the computational accuracy of the Simulink models. In addition, the rotation angle of the SC wall without the PT tendon appears to be monotonically increasing, indicating that the wall may topple over. On the contrary, the rotation angle of the SC wall firstly rises and then drops after the addition of the PT tendon, implying that in the case studied the PT tendon can effectively control the rotation and substantially improve the self-centering ability of the SC wall.

5.2. Influence of the Dampers. To investigate the influence of damper on the rocking response of the SC wall, another example is devised here. The parameters of the dampers are $f_y = 1.78\,\text{kN}$, $k_s = 10.0\,\text{kN/mm}$, and $\eta = 0.01$. Other parameters are identical with those listed in Table 1, except for that the 1940 El Centro N-S earthquake record is used alternatively. Figure 8 shows the accelerogram of the earthquake recording, in which the peak acceleration has been scaled to the same amplitude value as in the sine pulse excitation.

Figures 9 and 10 present the time history graphs of the rotation angle and angular velocity of the SC wall under seismic excitation, respectively, in which three different scenarios are considered, that is, (i) considering only the self-weight (without the PT tendon and dampers), (ii) adding only the PT tendon, and (iii) adding both the PT tendon and dampers. Figure 11 shows the hysteresis curve of the dampers.

It can be seen from Figure 9(a) that when considering solely the self-weight, the rotation angle of the SC wall goes up drastically and it overturns eventually at about 6 s since the rotation angle reaches nearly $\pi/2$; that is, the wall has already lain down on the ground. On the contrary, as shown in Figure 9(b), the rotation angle of the SC wall

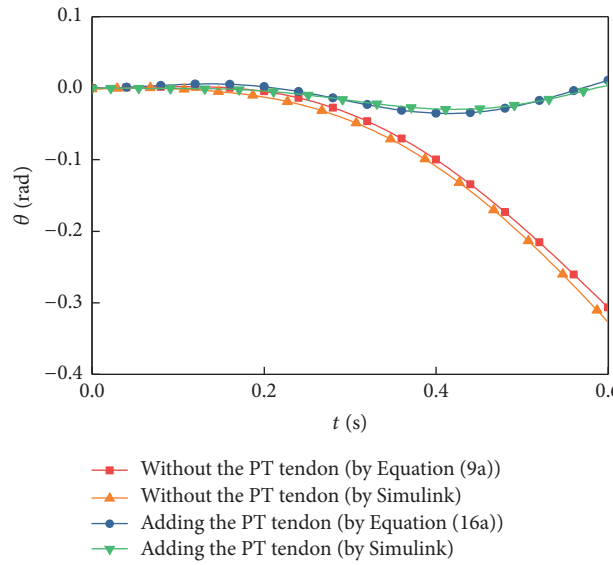

Figure 7: Effect of the PT tendon on the dynamic response of the SC wall.

including the PT tendon fluctuates around the zero axis and approaches virtually zero in the end. These observations are consistent with those discussed in Section 5.1, which further demonstrates that the PT tendon is capable of significantly improving the self-centering ability of the SC wall in the case studied.

From Figures 9(b) and 10, it can also be noticed that after the addition of the dampers, the rotation angle amplitude of the SC wall gets reduced remarkably from 0.035 rad to 0.015 rad, and the angular velocity amplitude drops from 0.56 rad/s to 0.37 rad/s. In addition, the time resetting the SC wall at the original position decreases significantly. This can be explained by the fact that the dampers consume a large amount of energy, as displayed in Figure 11, and thus improve

Table 2: Earthquake records used for the parametric study.

Number	Record	Distance to epicenter (km)	Duration (s)	PGA (cm/s^2)
EQ01	Loma Prieta, 1989, Gilroy	12	39.98	950.93
EQ02	North Palm Springs, 1986	6.7	59.98	967.61
EQ03	North Palm Springs, 1986	6.7	59.98	999.43
EQ04	Northridge, 1994, Sylmar	6.4	59.98	801.44
EQ05	Northridge, 1994, Newhall	6.7	59.98	664.93

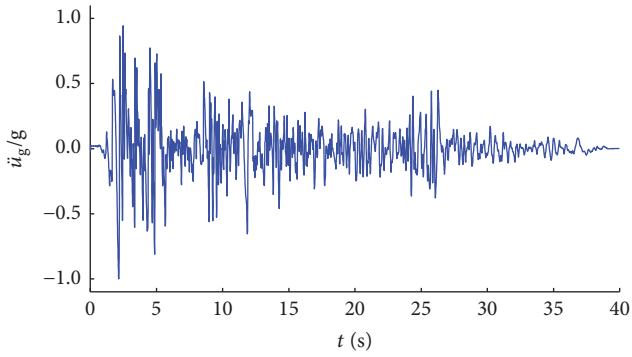

Figure 8: El Centro record.

the energy dissipation capacity of the SC wall. In addition, the computed hysteresis curve of the dampers is of bilinear shape, showing that the Simulink model developed in the paper can properly capture the hysteresis behavior of the dampers.

6. Parametric Study

6.1. Ground Motion Records. A parametric study is carried out in this section to further investigate the influence of a variety of parameters pertaining to the PT tendon and dampers on the dynamic response of self-centering walls under earthquake excitations. The geometry (h and b) and mass (m) of the SC wall are identical to those in Table 1. A suite of five real earthquake records, which were used by Somerville [38], are utilized for the parametric studies. The ground motion parameters for the utilized earthquake recordings are summarized in Table 2.

6.2. Effect of Parameters on the Dynamic Responses of the SC Wall

6.2.1. Effect of Parameters Pertaining to the PT Tendon. The parameters concerning the PT tendon include the initial force f_{p0} and the elastic stiffness k_p. In the parametric study, the two parameters are made variable while other parameters are set as constant throughout the study. For all the cases, the parameters concerning the dampers are kept unchanged as $f_y = 4.0$ kN, $k_s = 20$ kN/mm, and $\eta = 0.01$. It is noted that these parameter values are determined based on the given mechanical properties and geometry dimensions of the PT tendon and dampers.

Figure 12 shows the maximum rotation angle and angular velocity of the SC wall subjected to the selected earthquake ground motions for various values of f_{p0}. For all the cases, k_p is set to be 3.0 kN/mm. It can be found that for most of the records, the response amplitudes of the SC wall deceases remarkably with the increase of f_{p0}. For example, when subjected to the EQ02 ground motion, the peak values of the rotation angle and angular velocity of the SC wall for f_{p0} of 6.0 kN drop by 67 percent and 53 percent, respectively, as compared to those for f_{p0} of 1.0 kN. On the average, the values of the maximum rotation angle and angular velocity of the SC wall subjected to the selected records decrease by 69% and 50%, respectively, when the value of f_{p0} increases from 1.0 kN to 6.0 kN. On the basis of the above observations, it is concluded that increasing the initial force of the PT tendon considerably lessens the dynamic response of the SC wall in terms of rotation angle and angular velocity and thus enhances the self-centering ability of the SC wall.

Figure 13 shows the peak rotation angle and angular velocity of the SC wall subjected to the selected earthquake ground motions for various values of k_p considered in this study. For all the cases, f_{p0} is set to be 3.0 kN. Similar to the observations made earlier, the peak values of the rotation angle and angular velocity of the SC wall generally go down as k_p increases. On the average, the maximum values of the rotation angle and angular velocity of the SC wall decrease by 46 percent and 24 percent, respectively as k_p increases from 1.0 kN/mm to 8.0 kN/mm. Therefore, increasing the elastic stiffness of the PT tendon also seems to be effective in reducing dynamic response of the SC wall in terms of rotation angle and angular velocity, although it appears to be less effective than increasing the initial force.

6.2.2. Effect of Parameter concerning the Dampers. The parameters concerning the dampers involve the yield strength f_y and the elastic stiffness k_s, which, similar to the parameters in Section 6.2.1, will be taken as the variables during the parametric study. For all the cases, $\eta = 0.01$ and the parameters for the PT tendon are kept unchanged as $f_{po} = 3.0$ kN and $k_p = 3.0$ kN/mm.

Figure 14 presents the maximum rotation angle and angular velocity of the SC wall subjected to the selected earthquake ground motions for various values of f_y considered in this study. For all the cases, k_s is set to be 20 kN/mm. Different from the observations made in Figures 12 and 13, the peak values of the rotation angle and angular velocity of the SC wall for all the selected records plummet drastically as f_y

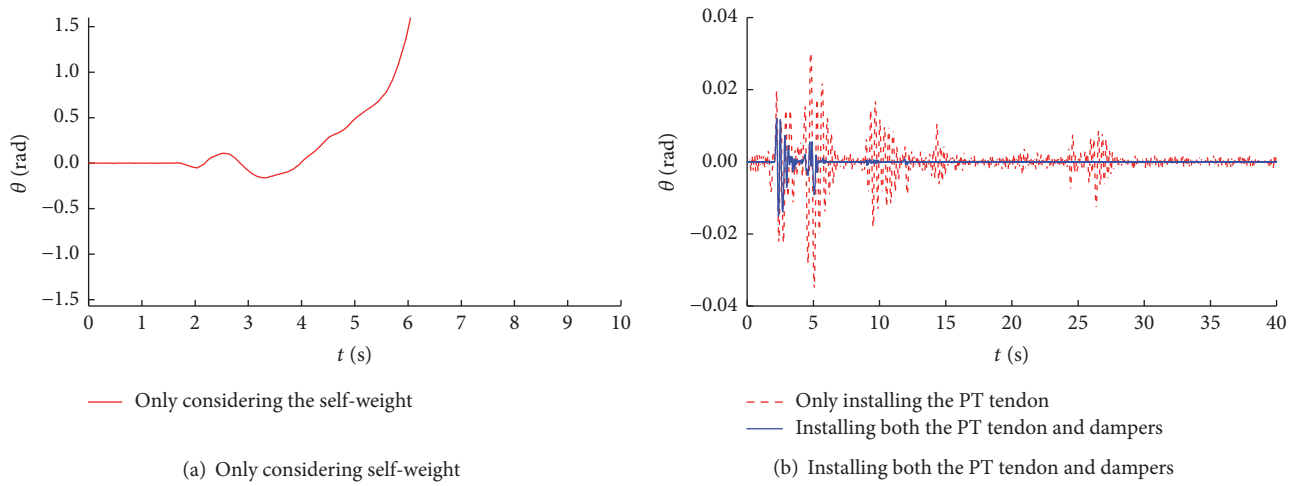

(a) Only considering self-weight

(b) Installing both the PT tendon and dampers

Figure 9: Rotation history curves of the SC wall under the ground excitation.

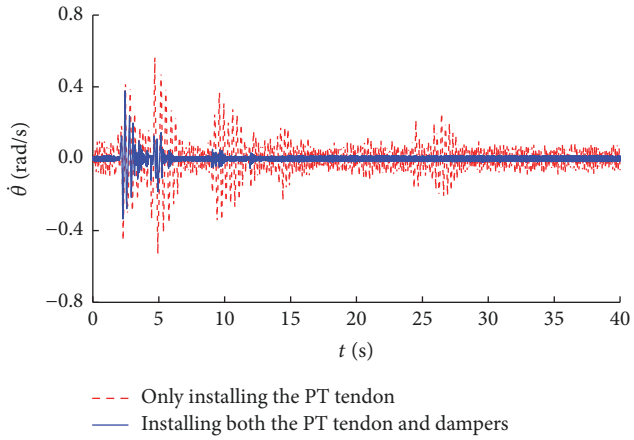

Figure 10: Angular velocity history curve of the SC wall after installing both PT tendon and dampers.

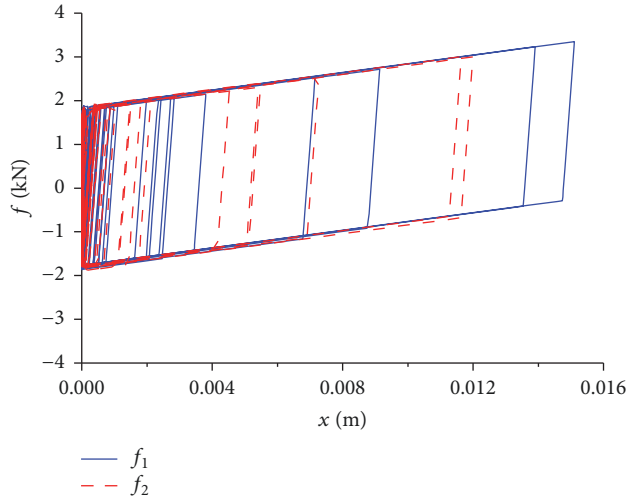

Figure 11: Hysteresis curves of dampers.

increases. Generally, the peak values of the rotation angle and angular velocity of the SC wall descend by 76 percent and 67 percent, respectively, as f_y ascends from 2.0 kN to 6.0 kN. This can be attributed to the fact that the dampers with a larger value of f_y consume more energy than those with a smaller f_y. These observations indicate that, instead of adjusting the parameters regarding the PT tendon, increasing the yield strength of the dampers appears to be a more reasonable and effective approach to lower the dynamic response of the SC wall.

Figure 15 shows the maximum rotation angle and angular velocity of the SC wall subjected to the selected earthquake ground motions for various values of k_s considered in this study. For all the cases, f_y is set to be 4.0 kN. It can be seen that, except for EQ02, the amplitudes of the rotation angle and angular velocity of the SC wall exhibit only slight variation with the increase of k_s. On the whole, the maximum values of the rotation angle and angular velocity of the SC wall decrease by 25 percent and 19 percent, respectively, as k_s increases from 10 kN/mm to 30 kN/mm. Based on the above observations, it can be inferred that the elastic stiffness of the dampers has a relatively insignificant effect on the dynamic response of the SC wall.

7. Conclusions

In this paper, assuming the SC wall as a rigid standing block, the equations of motion for different SC wall structural systems subjected to ground excitations are derived. After that, numerical simulations are then performed to examine the rocking response of SC walls under dynamic loading. In addition, parametric studies are also carried out to investigate the influence of a variety of factors on the dynamic response of SC walls. Within the cases studied in this paper, the following conclusions can be drawn:

(1) The PT tendon can considerably improve the self-centering ability of the SC wall. After equipping with the

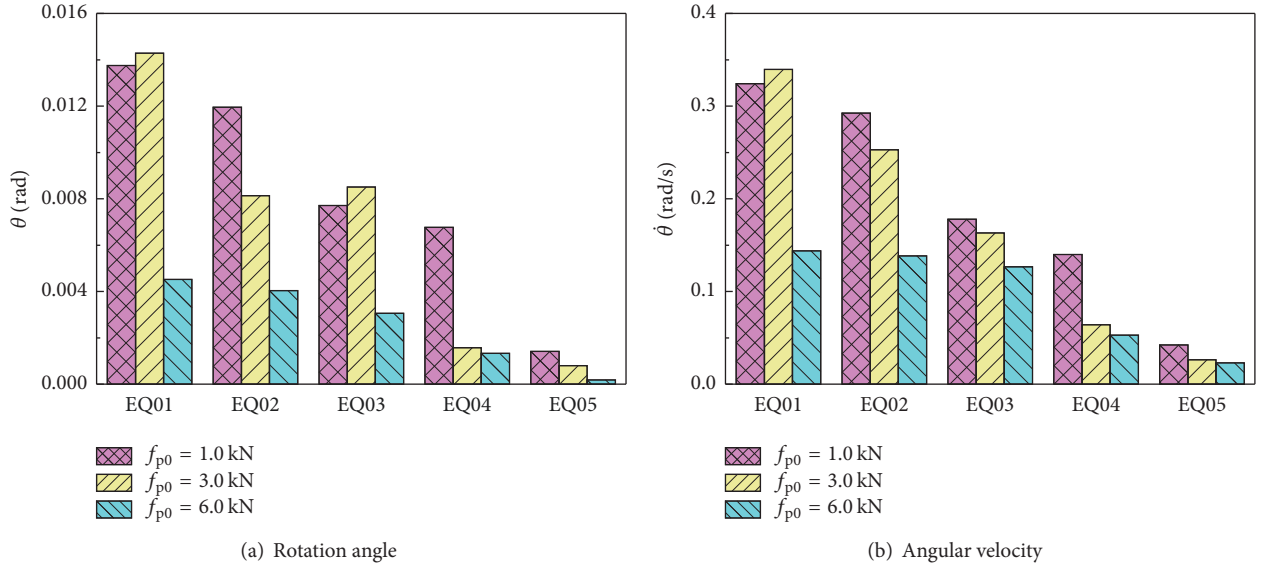

(a) Rotation angle (b) Angular velocity

Figure 12: Effect of f_{p0} on the dynamic responses of the SC wall.

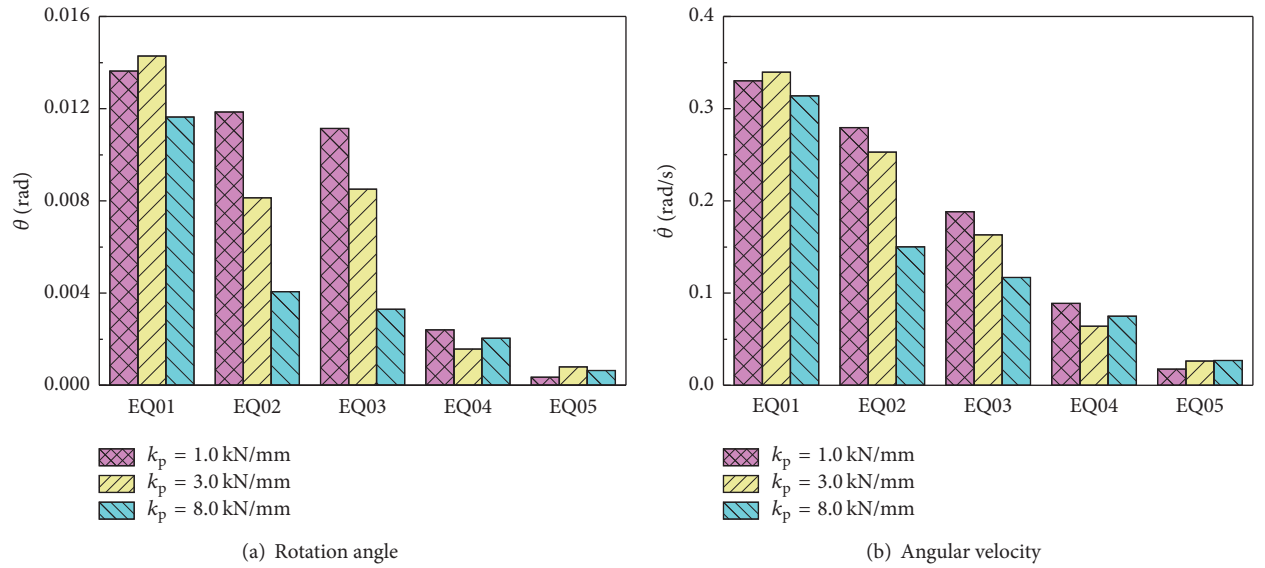

(a) Rotation angle (b) Angular velocity

Figure 13: Effect of k_p on the dynamic responses of the SC wall.

dampers, the energy dissipation capacity of the SC wall is substantially enhanced.

(2) Intensifying either the initial force or the elastic stiffness of the PT tendon is able to lower the dynamic response of the SC wall in terms of rotation angle and angular velocity, whereas the former approach is found to be more effective.

(3) It is shown that increasing the yield strength of the dampers appears to be a reliable and effective way of reducing the dynamic response of the SC wall, particularly in terms of rotation angle and angular velocity. On the other hand, the elastic stiffness of the dampers is observed to have a lesser impact on the dynamic response of the SC wall.

Disclosure

Any opinions, findings, and conclusions or recommendations expressed in this study are those of the authors and do not necessarily reflect the views of the National Science Foundation of China.

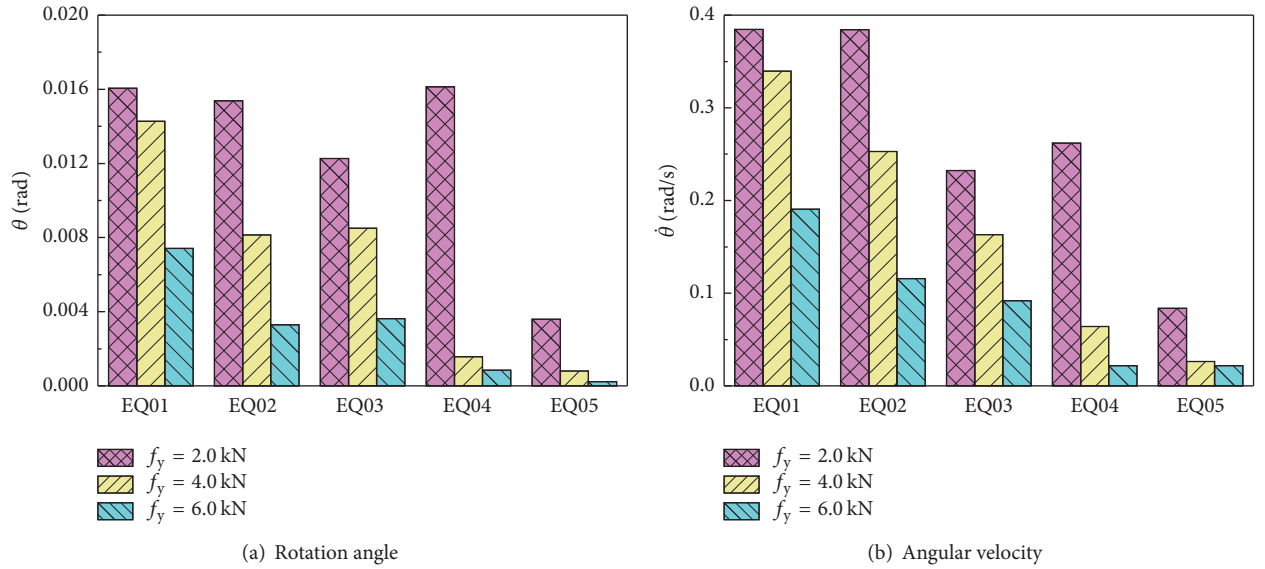

(a) Rotation angle (b) Angular velocity

Figure 14: Effect of f_y on the dynamic responses of the SC wall.

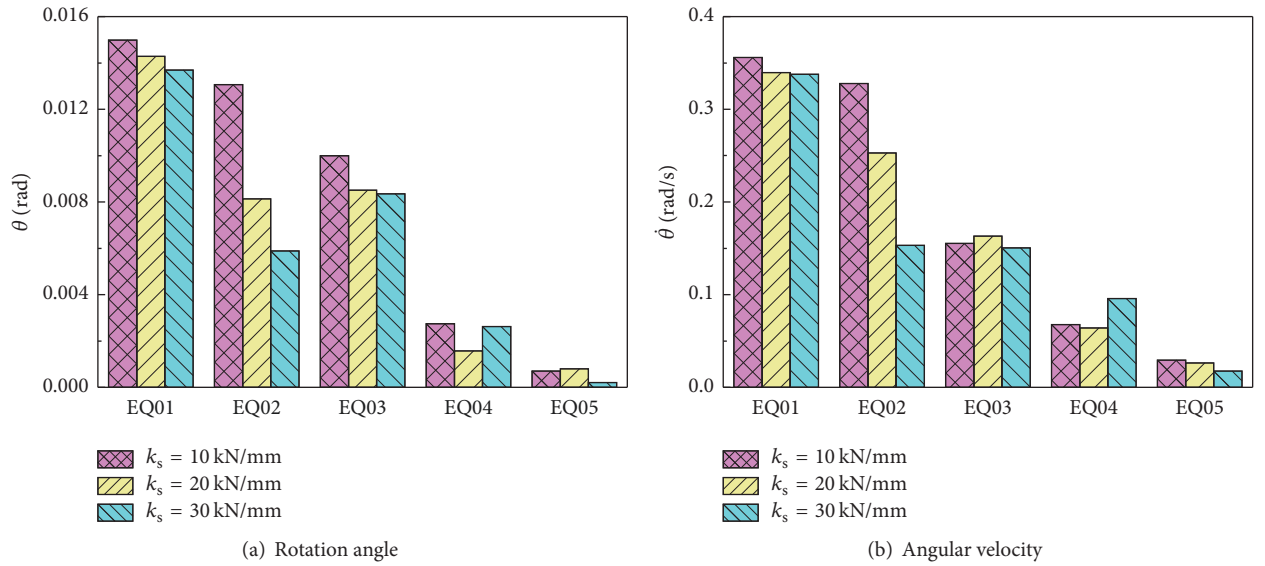

(a) Rotation angle (b) Angular velocity

Figure 15: Effect of k_s on the dynamic responses of the SC wall.

Conflicts of Interest

The authors declare that there are no conflicts of interest regarding the publication of this paper.

Acknowledgments

This research work was supported by the National Natural Science Foundation of China under Grant no. 51578429. The financial support is gratefully acknowledged.

References

[1] S. Pampanin, C. Christopoulos, and M. J. N. Priestley, "Performance-based seismic response of frame structures including residual deformations. Part II: multi-degree of freedom systems," *Journal of Earthquake Engineering*, vol. 7, no. 1, pp. 119–147, 2003.

[2] C. Christopoulos and S. Pampanin, "Towards performance-based seismic design of MDOF structures with explicit consideration of residual deformations," *ISET Journal of Earthquake Technology*, vol. 41, no. 1, pp. 53–73, 2004.

[3] M. T. El-Sheikh, R. Sause, S. Pessiki, and L.-W. Lu, "Seismic behavior and design of unbonded post-tensioned precast concrete frames," *PCI journal*, vol. 44, no. 3, pp. 54–71, 1999.

[4] C. Christopoulos, A. Filiatrault, and B. Folz, "Seismic response of self-centring hysteretic SDOF systems," *Earthquake Engineering & Structural Dynamics*, vol. 31, no. 5, pp. 1131–1150, 2002.

[5] M. Stevenson, L. Panian, M. Korolyk, and D. Mar, "Post-Tensioned Concrete Walls and Frames for Seismic-ResistanceA Case Study of the David Brower Center," in *Proceedings of the*

SEAOC 2008 Convention, pp. 1–8, Big Island, Hawaii, USA, 2008.

[6] C.-C. Chou and J.-H. Chen, "Column restraint in post-tensioned self-centering moment frames," *Earthquake Engineering & Structural Dynamics*, vol. 39, no. 7, pp. 751–774, 2010.

[7] J. F. Hajjar, M. Eatherton, X. Ma, G. G. Deierlein, and H. Krawinkler, "Seismic resilience of self-centering steel braced frames with replaceable energy-dissipating fuses-Part I: large scale cyclic testing," in *Proceedings of the Seventh International Conference on Urban Earthquake Engineering*, Tokyo, Japan, 2010.

[8] M. Preti and E. Giuriani, "Full scale experimental investigation on seismic structural walls," in *Proceedings of the Fifteenth World Conference on Earthquake Engineering*, Lisbon, Portugal, 2012.

[9] R. S. Henry, S. Sritharan, and J. M. Ingham, "Residual drift analyses of realistic self-centering concrete wall systems," *Earthquake and Structures*, vol. 10, no. 2, pp. 409–428, 2016.

[10] Y. C. Kurama, *Seismic analysis, behavior, and design of unbonded post-tensioned precast concrete walls*, Department of Civil and Environmental Engineering, Lehigh University, Bethlehem, PA, USA, 1997.

[11] Y. Kurama, S. Pessiki, R. Sause, L. W. Lu, and M. El-Sheikh, "Analytical modeling and lateral load behavior of unbonded post-tensioned precast concrete walls," NO. EQ-96-02, Department of Civil and Environmental Engineering, Lehigh University, Bethlehem, Pa., USA, 1998.

[12] Y. C. Kurama, "Seismic design of unbonded post-tensioned precast concrete walls with supplemental viscous damping," *ACI Structural Journal*, vol. 97, no. 4, pp. 648–658, 2000.

[13] F. J. Perez, *Experimental and Analytical Lateral Load Response of Unbonded Post-Tensioned Precast Concrete Walls*, Department of Civil and Environmental Engineering, Lehigh University, Bethlehem, Pa, USA, 2004.

[14] L. A. Toranzo, A. J. Carr, and J. I. Restrepo, "Improvement of traditional masonry wall construction for use in low-rise/low-wall-density buildings in seismically prone regions," in *Proceedings of the New Zealand Society for Earthquake Engineering 2001 Conference*, New Zealand, 2001.

[15] L. A. Toranzo, *The use of rocking walls in confined masonry structures: a performance-based approach*, University of Canterbury, Christchurch, New Zealand, 2002.

[16] A. Belleri, M. Torquati, and P. Riva, "Finite element modeling of "rocking walls"," in *Proceedings of the 4th International Conference on Computational Methods in Structural Dynamics and Earthquake Engineering, COMPDYN 2013*, pp. 2831–2848, Kos Island, Greece, June 2013.

[17] L. Panian, M. Steyer, and S. Tipping, "Post-Tensioned Concrete Walls for Seismic Resistance," *PTI Journal*, vol. 5, no. 1, pp. 7–16, 2007.

[18] J. I. Restrepo and A. Rahman, "Seismic performance of self-centering structural walls incorporating energy dissipators," *Journal of Structural Engineering*, vol. 133, no. 11, pp. 1560–1570, 2007.

[19] D. Pennucci, G. M. Calvi, and T. J. Sullivan, "Displacement-based design of precast walls with additional dampers," *Journal of Earthquake Engineering*, vol. 13, no. 1, pp. 40–65, 2009.

[20] B. Erkmen and A. E. Schultz, "Self-centering behavior of unbonded, post-tensioned precast concrete shear walls," *Journal of Earthquake Engineering*, vol. 13, no. 7, pp. 1047–1064, 2009.

[21] X. B. Hu, W. X. Li, H. Xiang, and H. G. He, "Study on the analysis model of the self-centering wall," *Applied Mechanics and Materials*, vol. 353-354, pp. 1850–1857, 2013.

[22] F. J. Perez, S. Pessiki, and R. Sause, "Experimental lateral load response of unbonded post-tensioned precast concrete walls," *ACI Structural Journal*, vol. 110, no. 6, pp. 1045–1055, 2013.

[23] B. J. Smith, Y. C. Kurama, and M. J. McGinnis, "Behavior of precast concrete shear walls for seismic regions: comparison of hybrid and emulative specimens," *Journal of Structural Engineering*, vol. 139, no. 11, pp. 1917–1927, 2013.

[24] L. Pakiding, S. Pessiki, R. Sause, and M. Rivera, "Lateral load response of unbonded post-tensioned cast-in-place concrete walls," in *Proceedings of the Structures Congress 2015*, pp. 1891–1902, Portland, Oregon, USA, April 2015.

[25] I. M. Qureshi and P. Warnitchai, "Computer modeling of dynamic behavior of rocking wall structures including the impact-related effects," *Advances in Structural Engineering*, vol. 19, no. 8, pp. 1245–1261, 2016.

[26] G. W. Housner, "The behavior of inverted pendulum structures during earthquakes," *Bulletin of the Seismological Society of America*, vol. 53, no. 2, pp. 403–417, 1963.

[27] S. J. Hogan, "The many steady state responses of a rigid block under harmonic forcing," *Earthquake Engineering & Structural Dynamics*, vol. 19, no. 7, pp. 1057–1071, 1990.

[28] W. K. Tso and C. M. Wong, "Steady state rocking response of rigid blocks part 1: Analysis," *Earthquake Engineering & Structural Dynamics*, vol. 18, no. 1, pp. 89–106, 1989.

[29] C. M. Wong and W. K. Tso, "Steady state rocking response of rigid blocks part 2: Experiment," *Earthquake Engineering & Structural Dynamics*, vol. 18, no. 1, pp. 107–120, 1989.

[30] J. Zhang and N. Makris, "Rocking response of free-standing blocks under cycloidal pulses," *Journal of Engineering Mechanics*, vol. 127, no. 5, pp. 473–483, 2001.

[31] N. Makris and J. Zhang, "Rocking response of anchored blocks under pulse-type motions," *Journal of Engineering Mechanics*, vol. 127, no. 5, pp. 484–493, 2001.

[32] L. Sorrentino, R. Masiani, and L. D. Decanini, "Overturning of rocking rigid bodies under transient ground motions," *Structural Engineering and Mechanics*, vol. 22, no. 3, pp. 293–310, 2006.

[33] A. Di Egidio, D. Zulli, and A. Contento, "Comparison between the seismic response of 2D and 3D models of rigid blocks," *Earthquake Engineering and Engineering Vibration*, vol. 13, no. 1, pp. 151–162, 2014.

[34] N. Makris and M. F. Vassiliou, "Dynamics of the Rocking Frame with Vertical Restrainers," *Journal of Structural Engineering (United States)*, vol. 141, no. 10, Article ID 04014245, 2015.

[35] M. F. Vassiliou and N. Makris, "Dynamics of the vertically restrained rocking column," *Journal of Engineering Mechanics*, vol. 141, no. 12, Article ID 04015049, 2015.

[36] L. D. Lutes and S. Sarkani, *Random Vibrations: Analysis of Structural and Mechanical Systems*, Elsevier Butterworth-Heinemann, Burlington, MA, USA, 2004.

[37] *Mathworks, MATLAB/Simulink*, 2006, https://www.mathworks.com/products/simulink.html.

[38] P. G. Somerville, "Development of ground motion time histories for phase 2 of the FEMA/SAC Steel Project," in *NO. SAC Joint Venture*, Calif, Sacramento, 1997.